



Forschungszentrum Karlsruhe
in der Helmholtz-Gemeinschaft

Wissenschaftliche Berichte
FZKA 6954

The CURVED Version of the Air Shower Simulation Program CORSIKA

D. Heck
Institut für Kernphysik

Februar 2004

Forschungszentrum Karlsruhe

in der Helmholtz-Gemeinschaft

Wissenschaftliche Berichte

FZKA 6954

The CURVED Version of the Air Shower Simulation Program CORSIKA

D. Heck

Institut für Kernphysik

Impressum der Print-Ausgabe:

**Als Manuskript gedruckt
Für diesen Bericht behalten wir uns alle Rechte vor**

**Forschungszentrum Karlsruhe GmbH
Postfach 3640, 76021 Karlsruhe**

**Mitglied der Hermann von Helmholtz-Gemeinschaft
Deutscher Forschungszentren (HGF)**

ISSN 0947-8620

Abstract

The CURVED Version of the Air Shower Simulation Program CORSIKA

This report describes the action of the *CURVED* version of the extensive air shower simulation program CORSIKA. The propagation of the shower particles in the ‘sliding planar atmosphere’ is described and the geometrical quantities used within the coding are derived.

Zusammenfassung

Die CURVED-Version des Luftschauer-Simulationsprogramms CORSIKA

Dieser Bericht beschreibt die Wirkungsweise der *CURVED*-Version des Programms CORSIKA zur Simulation ausgedehnter Luftschauer. Der Transport der Schauerpartikeln in der ‘gleitenden planaren Atmosphäre’ wird beschrieben, und die im Programm verwendeten geometrischen Größen werden abgeleitet.

Contents

1	Introduction	5
2	Sliding Planar Atmosphere	7
3	Coordinate System	9
3.1	Downward movement	9
3.2	Upward movement	10
4	The CURVED Routines	12
4.1	<i>COINC</i>	12
4.2	<i>NRANGC</i>	12
4.3	<i>PRANGC</i>	13
4.4	<i>THICKC</i>	13
4.5	<i>UPDATC</i>	13
4.6	<i>ELECTR</i> and <i>PHOTON</i>	14
4.7	Čerenkov routines	14
5	Final Tests	15
6	Acknowledgement	15
7	References	16

1 Introduction

When Extensive Air Showers (EAS) with moderate primary energy ($\approx 10^{15}$ eV) hit on ground arrays near sea level as KASCADE [1] at Forschungszentrum Karlsruhe, those EAS with very inclined incidence (zenith angle $\theta > 60^\circ$) are more or less completely absorbed within the atmosphere. For simulations in this energy range it is sufficient to restrict the shower incidence to $\theta < 60^\circ$ and to simplify the (in principle bent) atmosphere by planar layers neglecting the curvature of the Earth's surface. This is drawn schematically in Fig. 1.

With increasing energy and at elevated observation altitude very inclined EAS with zenith angles exceeding 60° will penetrate down to the Earth's surface. This is the case for the Pierre Auger Observatory [2] presently under construction at Malargüe, Argentina

In those cases the true atmosphere cannot be simplified any longer by a planar model, rather the finite Earth radius of 6371.315 km has to be taken into account, as represented in Fig. 2. In most EAS simulation programs (e.g. CORSIKA [3] and AIRES [4]) the altitude dependence of the atmospheric pressure is described by the U.S. standard atmosphere as parametrized by Linsley [5]. In this parametrization the altitude dependent density with barometric exponent is approximated within 4 layers in the altitude ranges 0 - 4 km, 4 - 10 km, 10 - 40 km, and 40 - 100 km. In a fifth layer above 100 km a linear decrease of the density with the altitude is assumed, which results in a finite range of the atmosphere with zero mass overburden at 112.8 km. All layers are parametrized in a manner to ensure smooth transitions in the density decrease as well as in the mass overlay when moving across a layer boundary. Tabulated values of this parametrization are reproduced in [6].

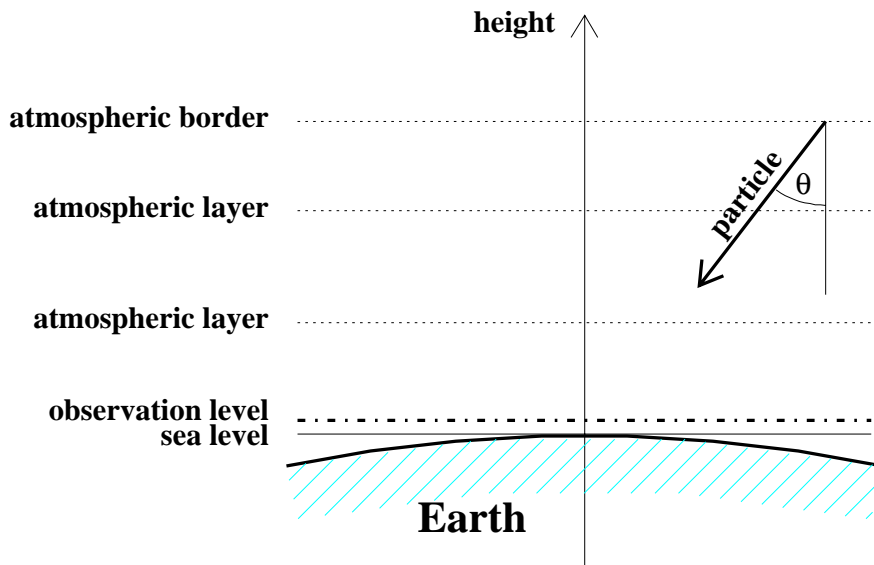


Figure 1: Flat geometry with planar atmosphere.

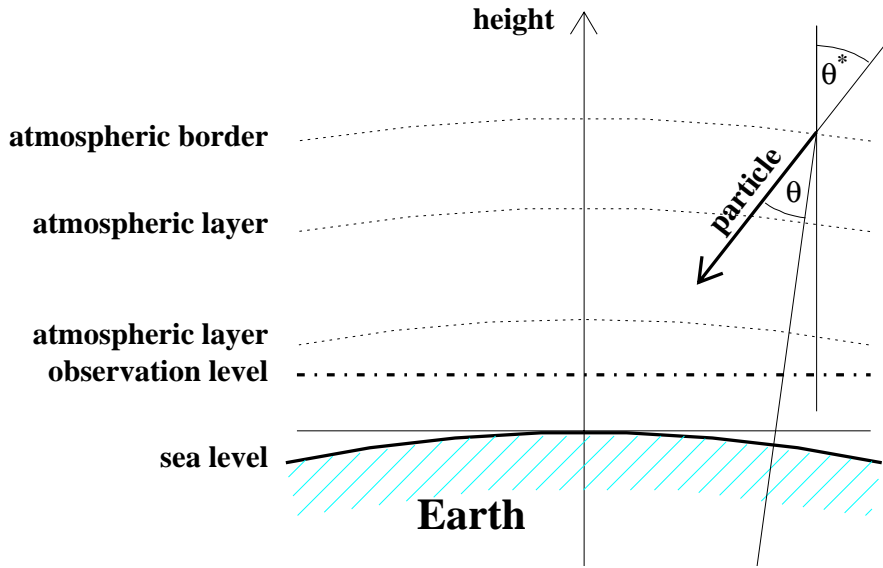


Figure 2: Curved geometry with bent atmospheric layers.

The influence of the Earth's curvature on the traveling distance from the atmospheric border to sea level and on the slant depth to be penetrated along this path is demonstrated in Table 1 for increasing zenith angles, which represent the angle of incidence at the observation level. Up to zenith angles of $\approx 70^\circ$ the differences in the penetrated matter of the planar and the spherical atmosphere remain below 1 %, but for zenith angles $> 70^\circ$ the differences become significant. This implies that the Earth's curvature cannot be neglected any longer in the simulation of EAS at extreme high primary energy and/or at high detection levels with large zenith angles.

zenith angle degree	planar		spherical	
	distance km	slant depth g/cm^2	distance km	slant depth g/cm^2
0	112.8	1036.1	112.8	1036.1
30	130.3	1196.4	129.9	1196.0
45	159.6	1465.3	158.2	1463.7
60	225.7	2072.2	220.1	2065.3
70	329.9	3029.4	310.7	3003.9
80	649.8	5966.7	529.0	5765.9
85	1294.6	11887.9	770.9	10572.1
89	6465.0	59367.2	1098.3	25920.4
90	∞	∞	1204.4	36481.8

Table 1: Distances and slant depths in planar and spherical geometry, calculated with the Linsley parametrization of the U.S. standard atmosphere.

2 Sliding Planar Atmosphere

The simulation of EAS in a true curved atmosphere needs a description of the particle propagation in an adequate coordinate system. A spheric coordinate system with its origin in the center of the Earth globe will do this best, but to get the penetrated matter along the (straight) particle path a numerical integration of the air density is needed for each particle transport. Such a procedure elongates the computing times in an intolerable manner. A different solution has been demonstrated with the AIRES code [4] which uses a so-called ‘sliding planar atmosphere’. This approach uses segments of planar atmospheres with all the simplicity of describing the transport of shower particles within them.

Each times when the movement of a shower particle exceeds a certain horizontal distance range, a transformation of the particle under consideration from one planar coordinate system into a new local planar atmosphere with horizontal layer boundaries is performed as indicated in Fig. 3. This is justified as long as the Earth’s curvature radius is large compared with the horizontal transport distances. Within the CORSIKA simulation package [3] with version number higher than 5.900 the bent atmosphere is realized in the *CURVED* option [7, 8] by a ‘sliding planar atmosphere’.

Let us assume the following notations as used in Fig. 3: In the first coordinate system the particle starts with a local zenith angle θ at the altitude \mathbf{h} . It is transported over a horizontal distance \mathbf{r} and arrives at the altitude \mathbf{h}' , where it changes over to the next planar coordinate system rotated by the angle δ , so in the new system the particle gets the zenith angle θ'' with the relation $\theta'' = \theta + \delta$. The new altitude \mathbf{h}'' will be larger than \mathbf{h}' and hence the mass overlay $thick(\mathbf{h}')$ will change to $thick(\mathbf{h}'') < thick(\mathbf{h}')$

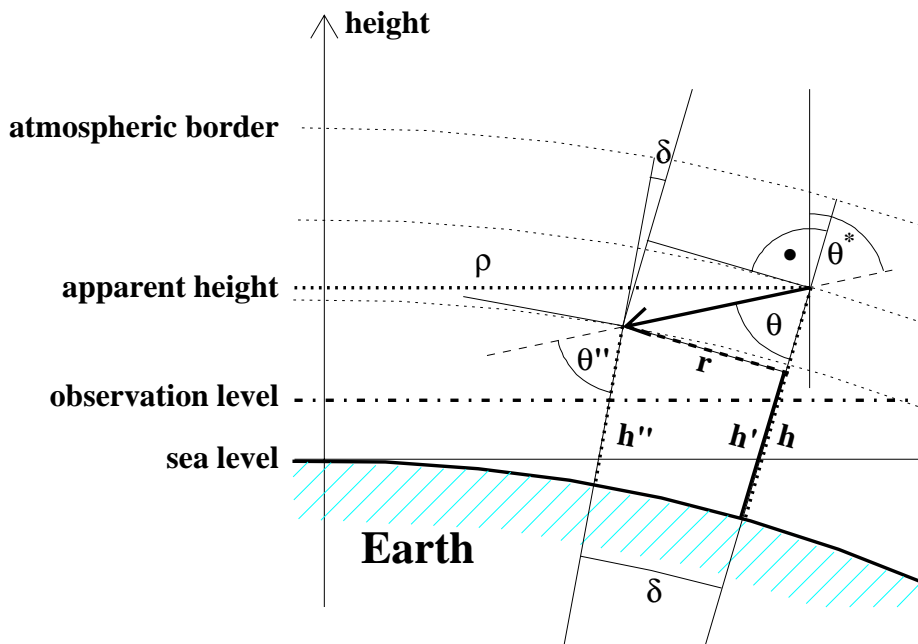


Figure 3: Particle in curved geometry.

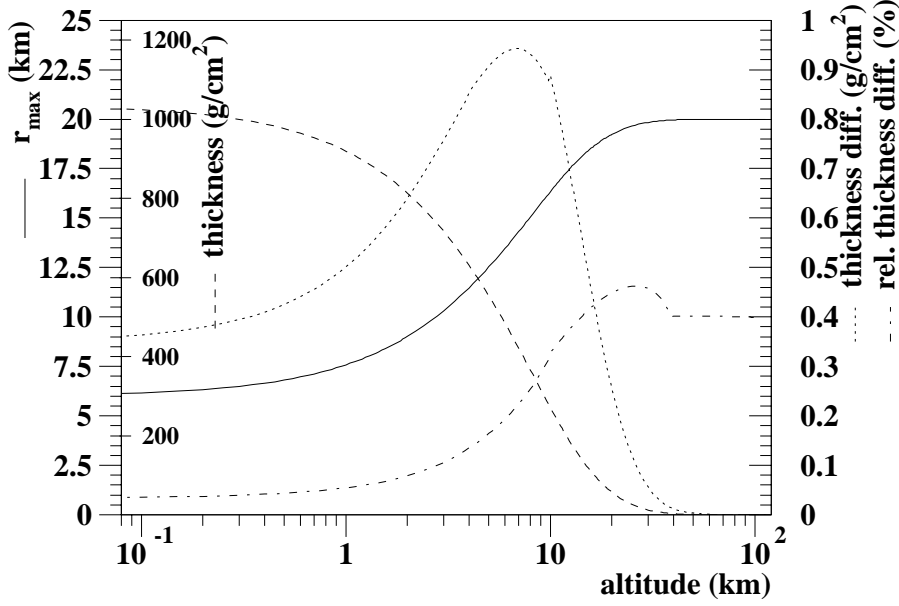


Figure 4: Altitude dependence of maximum horizontal transport distance (solid line), thickness (dashed line), relative thickness difference at maximum transport distance (dotted line), and absolute thickness difference at maximum transport distance (dashed-dotted line).

in a jump which depends on the length of the horizontal movement \mathbf{r} . This jump can be hold small enough, if the free horizontal movement \mathbf{r}_{\max} is restricted in a suitable manner, dependent on the altitude of the particle. Within CORSIKA the free horizontal movement is limited by

$$\mathbf{r}_{\text{sea}} = 6 \text{ km} \text{ at sea level with mass overlay } \mathit{thick}(0),$$

$$\mathbf{r}_{\text{toa}} = 20 \text{ km} \text{ at top of atmosphere with vanishing mass overlay } \mathit{thick}(\mathbf{h}_{\text{toa}}) = 0.$$

In the altitude \mathbf{h} between these extrema an interpolation is performed:

$$\mathbf{r}_{\max} = \frac{\mathbf{r}_{\text{toa}} - \mathbf{r}_{\text{sea}}}{\mathit{thick}(0)} \cdot \mathit{thick}(\mathbf{h}) + \mathbf{r}_{\text{sea}}. \quad (1)$$

Using these restrictions with the U.S. standard atmosphere, at a transition from one local planar system to the next one the relative difference in thickness remains below 0.5 % (with a maximum of $< 0.47\%$ at 26 km altitude) for the layers with exponential density decrease. This is shown in Fig. 4. The absolute differences in mass overlay steps stay below 1 g/cm^2 reaching a maximum of $< 0.95 \text{ g/cm}^2$ at an altitude of 7 km. If the horizontal component of a particle path becomes longer than \mathbf{r}_{\max} , the path is chopped in segments which fulfil the horizontal movement restrictions.

For each transition into a new local coordinate system the horizontal coordinates have to be corrected, as the projection of the actual position down to the Earth surface will be rotated by the angle δ , too, which results in an approximate horizontal distance correction by

$$\Delta \mathbf{r} = \mathbf{h}'' \sin \delta \approx \mathbf{h}'' \delta.$$

3 Coordinate System

Deviating from the standard CORSIKA version where the horizontal coordinates \mathbf{x} and \mathbf{y} have their origin in the point of the first interaction (or eventually in the primary's entering point at the top of atmosphere), in the *CURVED* version the origin is placed at the center of the observation level. The orientation relative to North remains unaffected, as well as the zero reference altitude is kept unchanged at sea level.

3.1 Downward movement

When starting the primary at the top of atmosphere, the \mathbf{x} and \mathbf{y} coordinates of the starting point are calculated in a manner that the flight path points to the center of the observation level with the selected zenith angle θ^* and the azimuthal angle φ . The exact horizontal distance is calculated along the Earth surface as

$$\mathbf{r} = \mathbf{R}_E \cdot \theta_E \quad (2)$$

where \mathbf{R}_E is the Earth radius. The cosine of the angle θ_E is obtained from geometrical relations using the apparent height, see Fig. 5.

The distances \mathbf{A}_1 , \mathbf{A}_2 , and $\mathbf{R}_E + \mathbf{Obs}$ form a rectangular triangle. A second rectangular triangle is built up from \mathbf{A}_2 , $\mathbf{A}_1 + \mathbf{DIAG}$, and $\mathbf{R}_E + \mathbf{h}$. Using the Pythagorean relationship for this second triangle and replacing \mathbf{A}_1 by

$$\mathbf{A}_1 = (\mathbf{R}_E + \mathbf{Obs}) \cdot \cos \theta^*$$

results in the distance

$$\mathbf{DIAG} = \sqrt{(\mathbf{R}_E + \mathbf{h})^2 - (1 - \cos^2 \theta^*) \cdot (\mathbf{R}_E + \mathbf{Obs})^2} - (\mathbf{R}_E + \mathbf{Obs}) \cdot \cos \theta^*. \quad (3)$$

The height difference between the apparent height and the observation level is given by $\mathbf{DIAG} \cdot \cos \theta^*$, so finally $\cos \theta_E$ may be written as

$$\cos \theta_E = \frac{\mathbf{R}_E + \mathbf{Obs} + \mathbf{DIAG} \cdot \cos \theta^*}{\mathbf{R}_E + \mathbf{h}}.$$

These calculations are performed each times the local planar coordinate system is changed following the transport step of a particle. Using eq. 2 the distance of a particle to the center of the observation level is easily monitored. When a particle approaches the coordinate origin and comes closer to it than \mathbf{r}_{\max} , the particle's coordinates are transformed from the actual coordinate system into the Cartesian system of the observation level.

By choosing the coordinate system in this manner the handling of more than one observation level becomes extremely complicated. Therefore in the *CURVED* version the number of observation levels is restricted to one.

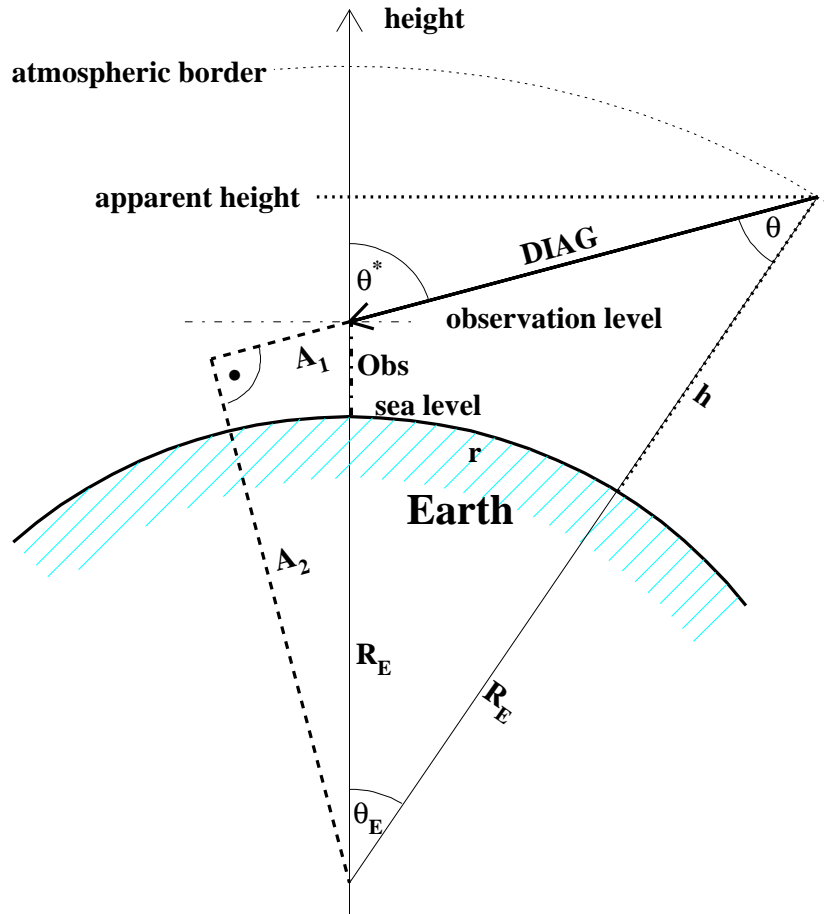


Figure 5: Downward movement in curved geometry.

3.2 Upward movement

By the transverse momentum of hadronic interactions and/or by multiple scattering especially of the leptons sometimes in nearly horizontal showers particles might go upwards. From each annihilation one of the two 511 keV γ -quanta will move upwards by kinematical reasons.

A different problem arises for those EAS, which originate e.g. from upward going τ -leptons. These τ -leptons are generated by the charged-current interaction of ν_τ -neutrinos close below the Earth surface after having penetrated the whole globe. The τ -leptons decay in the atmosphere and the decay products generate an EAS. For those showers we cannot expect any registration in surface array detectors. Rather by the emission of fluorescence photons they may be detected in ground-based set-ups like the High Resolution Fly's Eye [9] or the Pierre Auger Observatory [2] experiment or from space by satellites like EUSO [10] and OWL [11].

If the primary particle is already moving upward as indicated in Fig. 6, an observation level must be defined at the top of the atmosphere. Similarly to eqs. 2 - 3 we get

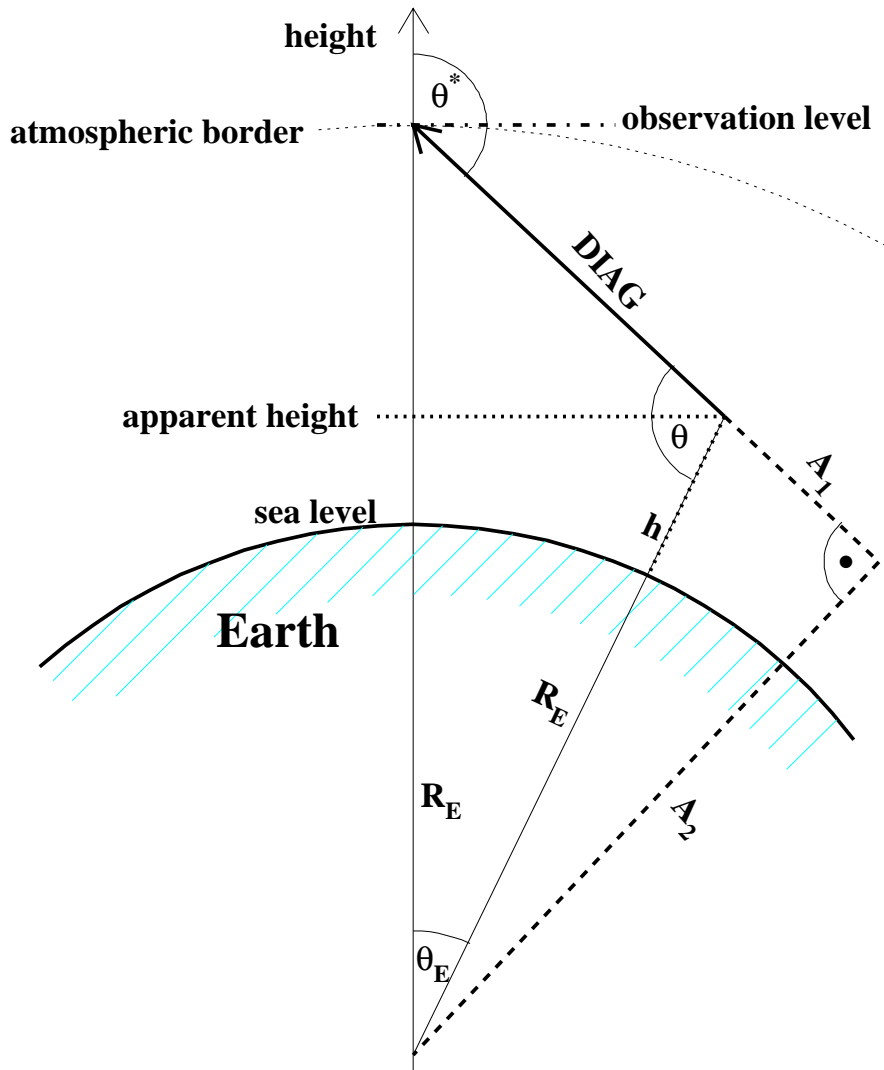


Figure 6: Upward movement in curved geometry.

for the distance **DIAG** the expression

$$\mathbf{DIAG} = -\sqrt{(\mathbf{R}_E + \mathbf{h})^2 - (1 - \cos^2 \theta^*) \cdot (\mathbf{R}_E + \mathbf{Obs})^2} - (\mathbf{R}_E + \mathbf{Obs}) \cdot \cos \theta^*$$

which differs from eq. 3 only in the negative sign ahead of the square root.

4 The CURVED Routines

To realize the concept of the sliding planar atmosphere a series of routines had to be modified or new routines had to be written, which are described in this section. In the *CURVED* version three additional parameters of each particle are stored in the particle stack:

- **happ**, the apparent height giving the height in the Cartesian detector system,
- **costap**, the cosine of the particles apparent zenith angle in the Cartesian detector system $\cos\theta^*$,
- and **costea**, the cosine of the angle between the particle projection and the projection of the detector middle to the center of Earth $\cos\theta_E$.

These quantities are needed when changing from one planar system to the next one. They are updated after each particle movement.

4.1 COOINC

The coordinate system is initialized in a manner that the origin of the horizontal coordinates coincides with the center of the observation level. The altitude is counted from sea level upward. The coordinates of a primary particle entering into the atmosphere are calculated in the subroutine COOINC as described in section 3. The cosine of the actual zenith angle $\cos\theta$, the apparent height, and the $\cos\theta_E$ are determined using the Earth radius \mathbf{R}_E , the height of the observation level \mathbf{Obs} , the altitude \mathbf{h} of the top of atmosphere, and the cosine of the selected zenith angle $\cos\theta^*$ (see Fig. 5).

4.2 NRANGC

For decaying particles the transport path length is determined by the decay time. For a given path length and direction the traversed matter thickness is calculated for decaying neutral particles in the subroutine NRANGC. The path is chopped in pieces with a length according eq. 1 and the traversed mass thickness $\Delta\chi$ in a segment is determined from the starting altitude \mathbf{h} with mass overburden $thick(\mathbf{h})$ and the altitude difference $\Delta\mathbf{h}$ within this segment to

$$\Delta\chi = \frac{thick(\mathbf{h} - \Delta\mathbf{h}) - thick(\mathbf{h})}{\cos\theta}.$$

The total traversed mass thickness χ is formed by summation over the individual pieces $\Delta\chi$.

4.3 *PRANGC*

For charged particles with a path length determined by their life time the calculation of the traversed matter is more complicated, as in each segment additionally the ionization energy loss is taken into account. The shortening of the free path of decaying particles by the ionization energy loss is treated for planar atmospheres in the subroutine PRANGE. The routine PRANGC used with the *CURVED* version is an adaptation to the segmented transport respecting the ionization energy loss at each step. After each segment the Lorentz γ -factor and the particle velocity β (in units of the velocity of light) have to be recalculated. Special attention has to be given to a transition across atmospheric layer boundaries, which results in a nested chopping of the total path.

Both routines NRANGC and PRANGC are used only for those particles, which eventually will decay at the end of the transport path, to get the penetrated matter thickness for decay. This is needed for a comparison with the penetrated matter in case of interaction, and the shorter of both decides the future fate of the particle under consideration.

4.4 *THICKC*

The function THICKC is called from the CORSIKA main program to find the point of the first interaction and its mass overburden for hadronic and muonic primaries. These particles will traverse the matter thickness χ_c and not undergo decay. Ionization energy loss, multiple scattering, and deflection in the Earth magnetic field are neglected for the calculation of the estimated arrival point. The path to this point is chopped with the maximum horizontal transport length according eq. 1 and after each segment the remaining matter thickness χ_c is reduced by the matter χ_n traversed in the segment under consideration. The path length χ_n of the last segment is reduced to the remaining thickness χ_c .

4.5 *UPDATC*

The transport of a particle in a curved coordinate system is performed in the subroutine UPDATC by chopping its path. This routine handles the transport across each segment by calling the routine UPDATE which describes the transport in a planar atmosphere, respecting multiple scattering, ionization energy loss and deflection in the Earth magnetic field. The approach of the particle to the observation level is monitored in UPDATC by comparing the particle height with the altitude of the observation level. If at the end of the (planar) transportation segment the height h' becomes lower than the observation level, a transition into the Cartesian system of the detector is performed. The apparent height and the distance from the detector center are used to calculate the angle δ by which the local planar system has to be rotated to come into the detector system.

4.6 *ELECTR* and *PHOTON*

In the EGS4 part of CORSIKA the transportation step is limited in subroutine HOWFAR to the maximum free path in horizontal directions according to eq. 1. HOWFAR also checks whether the em-particle will reach the detector level within the next (limited) step and indicates this by a negative flag IDISC. In this case the routines ELECTR resp. PHOTON transform the particle coordinates in an appropriate manner into the Cartesian frame of the detector before the particle is transported to the detector.

If the em-particle is far away from reaching the detector the transition into a new local planar system is performed after the transport step. These transitions include the correction of the direction cosines \mathbf{u} , \mathbf{v} , and \mathbf{w} (because of the rotation of the reference system by the angle δ), the horizontal coordinates \mathbf{x} and \mathbf{y} as well as the vertical altitude \mathbf{z} .

If the transport occurred to the first interaction point (as the em-particle is the primary particle), the subroutine CORNEC is called which initializes the position coordinates and direction cosines at the interaction point relative to the middle of the detector, see section 3.

4.7 Čerenkov routines

The treatment of Čerenkov photons in subroutine CERENK differs from the transport of particles by other routines of the *CURVED* option in so far as the Čerenkov photon coordinates of the emission point are transformed immediately to the Cartesian system of the detector, as no interactions within the atmosphere are regarded. Special care is taken to get the propagation distance and time correctly. For this purpose in the subroutine INRTAB the two-dimensional tables DISTEF (effective distance) and TOF (time of flight) are initialized as functions of the emission height above the observation level plane and of the emission angle relative to this plane. These tables are used afterwards in the functions DISTIP and TOFIP for interpolations.

For a given emission height and emission zenith angle DISTIP calculates the distance between the point of Čerenkov emission and the observation level. It takes into account the refractive index of air, which becomes important for very inclined emission where the light propagates no longer in an exact straight line but rather in a slightly bent curve caused by the increase of the refractive index with decreasing altitude.

Similarly TOFIP calculates the time of flight between the Čerenkov emission and arrival at observation level. Again for very inclined emission the elongation of the transport time by the slightly curved light path and the varying refractive index is respected in the calculations.

5 Final Tests

A comparison of simulations performed at $\theta = 70^\circ$ for hadrons and muons with the planar (standard) and with the *CURVED* version revealed an increase of CPU time by $\approx 30\%$.

The validity of the coordinate transformations at the segment boundaries has been checked by the deviation of the trace of a 1 PeV muon from the detector center after penetrating the complete atmosphere. Any muonic interaction, magnetic deflection, or multiple scattering had been switched off for this test. This muon impinged on the detector with $\theta = 89^\circ$ after a horizontal transport over a distance of ≈ 1100 km corresponding with a movement over 10° degrees along an Earth's meridian. For this path length the muon had to be transported through more than 100 segments of planar atmosphere including the corresponding transformations at the boundaries of the segments. The test revealed a missing of the detector center by $< .0003$ mm caused by rounding errors in the double precision calculations.

6 Acknowledgement

The engagement of F. Schröder (Wuppertal) in programming and modifying the routines for the *CORSIKA-CURVED* version, especially for the Čerenkov propagation, and in testing the developed *CORSIKA* modifications is acknowledged.

References

- [1] T. Antoni et al., KASCADE Collaboration, *Nucl. Instr. Meth. A* **513** (2003) 490
- [2] P. Auger Collaboration, *Pierre Auger Design Report*, Fermilab (1997), <http://www.auger.org/admin/DesignReport/index.html>
- [3] D. Heck et al., Report **FZKA 6019** (1998), Forschungszentrum Karlsruhe; http://www-ik.fzk.de/~heck/corsika/physics_description/corsika_phys.html
- [4] S.J. Sciutto, preprint astro-ph/9911331 (1999); Auger technical note **GAP-98-032** (1998), http://www.auger.org/admin-cgi-bin/woda/gap_notes.pl; for an up-to-date version see <http://www.fisica.unlp.edu.ar/auger/aires>
- [5] J. Linsley, private communication by M. Hillas (1988)
- [6] J. Knapp and D. Heck, Report **KfK 5196B** (1993), Kernforschungszentrum Karlsruhe; for an up-to-date version see http://www-ik.fzk.de/~heck/corsika/usersguide/corsika_tech.html
- [7] D. Heck, F. Schröder, KASCADE Collaboration, *Proc. 26th Int. Cosmic Ray Conf.*, Salt Lake City (USA) **1** (1999) 498
- [8] F. Schröder, Diss. Universität Wuppertal (2001); Report **WUB-DIS 2001-17** (2001), Universität Wuppertal; <http://elpub.bib.uni-wuppertal.de/edocs/dokumente/fb08/diss2001/schroeder/f080105.pdf>
- [9] T. Abu-Zayyad et al., HiRes Collaboration, submitted to *Astropart. Phys.* (2003); preprint astro-ph/0208301 (2002)
- [10] L. Scarsi et al., *EUSO - Extreme Universe Space Observatory*, Proposal for the ESA F2/F3 Mission; O. Catalano, *Il Nuovo Cimento* **24C** (2001) 445; <http://euso.riken.go.jp>
- [11] L. Scarsi et al., *Proc. 26th Int. Cosmic Ray Conf.*, Salt Lake City (USA) **2** (1999) 384; <http://owl.gsfc.nasa.gov>